

In-situ computer tomography for analyzing the effect of voids on the damage behavior of composite materials

R Protz*, I Koch and M Gude

TU Dresden, Institute of Lightweight Engineering and Polymer Technology (ILK),
Holbeinstr. 3, 01307 Dresden, Germany

* richard.protz@tu-dresden.de

Abstract. Due to their high specific stiffness and strength composites are ideally suited for applications in machine building, vehicle constructions, wind power technology and aviation. In the manufacture of composite structures voids are an unavoidable fact. Several non-destructive techniques are potentially able of detecting defects, but only the exact knowledge of the effects of defects on the mechanical properties allows the definition of thresholds for the purpose of quality management. Here, an experimental program for characterizing the effect of voids on the damage behaviour is presented. Flat specimens with glass fibre non-crimp fabric reinforcement and epoxy matrix (GF-NCF/EP) are produced using vacuum assisted resin transfer moulding. By means of a specific adjustment of the process parameters, test specimens with three different void contents are produced and compared. For detailed analysis of damage evolution in the vicinity of voids, in-situ computed tomography (in-situ CT) is used, for the volumetric visualization of the material during tensile loading.

1. Introduction

Composites offer high levels of specific stiffness and strength as well as an adjustable energy absorption capacity. Thus, they are ideally preferred for applications in material and energy efficient lightweight structures as used in the wind energy utilization and in aviation [1, 2]. In the manufacture of composite structures voids of different size, geometry and orientation are an unavoidable fact [3, 6-10] and have been investigated by many authors. Investigations can be divided in studies on the mechanism of void formation [10-17] and in studies on the effect of voids on the mechanical behavior [3, 6-8].

The development of voids strongly depends on the manufacturing technology. The cause of voids in prepreg materials used in the autoclave process differs essentially from that of semi-finished products infiltrated in an infusion process [18]. Voids are formed in a prepreg laminate when the pressure applied to the liquid resin is lower than the opposing vapor pressure of moisture entrapped in the laminate [22, 23]. Investigations to void formation and void morphology in prepreg materials were published among others in Refs. [7, 8, 10, 19-24]. Prepreg materials are commonly used for investigating the influence of voids on the subsequent material behavior. During the infusion process (i.e. the various resin transfer moulding process, RTM), the resin is injected in a mould cavity containing the textile preform. The interaction of vacuum quality, pressure of resin-injection, permeability of the reinforcement material and viscosity of the resin all show major influences on content and phenomenology of the emerging voids. These parameters lead to variations of the flow rate in the fibre bundles and in the channels



between two bundles. Different flow fronts of the resin support a partial infiltration leading to void encapsulation.

In the literature there are indications of a critical void contents from which an influence of the mechanical properties are identifiable in the range from 0.3 % to 6 % [20-22, 25-27]. This wide range results from the fact that apart from the pure void content, especially the size, the shape and the distribution of the voids as well as the type of load must be considered.

For the determination of void contents, void geometry and for the analysis of the influence of voids during mechanical loads, a large number of test methods such as microscopy, ultrasound technology, thermography, acoustic emission analysis and X-ray methods are already available. In order to avoid destruction of the non-transparent samples, void analysis under the microscope is limited to the cover layers and the longitudinal edges of the specimens [33, 34]. Under mechanical stress, voids can be detected by ultrasound or thermally excited lock-in thermography [35]. Also acoustic emission is often used for determining the effect of voids in composites on the damage behaviour [36]. With in-situ CT it is possible to efficiently analyse void content and morphology of voids and the influence of voids under static loading. As published in [32], the existing disadvantages of classical CT-based damage analysis, such as stress-strain-hysteresis effects, inaccuracies due to crack-closing phenomena after specimen relief and damage induction due to repeated expansion and contraction, are eliminated with this method. This also significantly reduces the experimental effort.

The focus in this paper is a detailed analysis of damage evolution in the vicinity of voids. The generated void volume levels in these studies were between 0.01 % and 2.9 % (as well as in the investigations of other authors) and thus typical for composites produced in resin transfer moulding process [6, 10-17, 25-29]. Praxis related glass fibre non crimp fabric reinforced epoxy composite (GF-NCF/EP) was considered. More detailed results of the author's studies on the influence of voids in the aforementioned material regarding its structural behaviour have been published in Refs. [5, 30, 31].

2. Specimen preparation

For the experimental and theoretical studies, composites with GF-NCF reinforcement of eight layers [90/-45/0/45/-45/0/45/90] are considered. The plies contain different amount of fibers (49 % in 0°, 23 % in -45°, 23 % in 45 and 5 % in 90°).

Using the vacuum assisted resin transfer moulding (VARTM) method, test plates were infiltrated in a flat steel mould with injection epoxy resin (EP) RIMR 135 with hardener RIMH 137 in a ratio of 100:30. This resin has a low viscosity and is cold curing within 24 h. For the purpose of reducing the process time, the infiltration as well as curing is carried out at 40 °C. A curing time of 10 h is followed by a tempering cycle of 6 h at 80 °C. After the heat treatment the resin shows a glass transition temperature of 85 °C. A volume fraction of about 33 % has been achieved according to ISO 1172.

To investigate the influence of production-related defects, voids with contents of 0.01 %, 1.43 % and 2.9 % have been systematically induced by adapted process parameters and modified VARTM-complex. The main influencing parameters for adjusting the void contents are the injection pressure on the sprue side and the vacuum pressure on the riser side, as this can vary the resin flow rate.

After infiltration and hardening test specimens with dimensions of 100 mm in length, 15 mm in width and 3 mm in thickness were cut from the test plate with water cooled diamond-tipped saw blade (Figure 1). In order to prevent failure caused by the fixing of the test machine aluminium-doublers on both ends of the flat specimen are used. This results in a free test length of 70 mm.

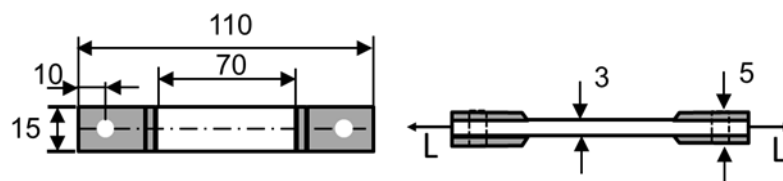


Figure 1. Geometry of the test specimens (dimensions in mm)

3. Test equipment and procedure

An in-situ computer tomograph (in-situ CT) is used for detailed analysis of the evolution of damage caused by voids under superimposed tensile loading at the micro level (Figure 2). This unique test complex consists of a tensile-compression torsion testing machine with a maximum force of 250 kN and a maximum torque of 2000 Nm and a computer tomograph FCTS 160-IS from Finetec, whose technical performance data are shown in Table 1. The right side of Figure 2 shows the alignment of the load train between the X-ray source and detector rotating around the loaded sample during the scan cycle. The measuring time is approx. 20 min at a resolution of 6.3 μm .



Figure 2. In-situ CT test rig (left) and test unit (right)

Table 1. Technical performance data of the in-situ CT test complex

Parameter	Characteristic
Acceleration voltage	30 - 160 kV
X-ray current	10 - 1000 μA
Target material	Tungsten
Min. focal spot	3 μm
Active detector area	405 mm x 290 mm
Detector resolution	3200 x 3200 pixels
Grayscale	14 bit
Min. measuring field diameter	85 mm
Max. Measuring field height	60 mm

Figure 3 shows the basic procedure of an in-situ CT examination on test specimens. Immediately after the specimen has been clamped, a first load-free scanning cycle takes place, which analyses the existing voids in the specimen. Then, analogous to quasi-static tensile tests, the force is measured continuously at a test speed of 2 mm/min until a force drop of 0.2 % of the current force is registered on the machine side. This indicates an increase in damage. The testing machine automatically relieves the load to 50 % of the force in the peak and remains force-controlled in the second scan cycle. After a waiting time of 90 seconds for strain retardation in the material, the CT scan starts. Within 20 minutes, the X-ray unit rotates around the sample and tomographs the damage. In the next step, the specimen is loaded in position control until another force drop occurs and the third scan cycle starts in force control at 50 % of the current force peak. These processes are repeated until the specimen fails.

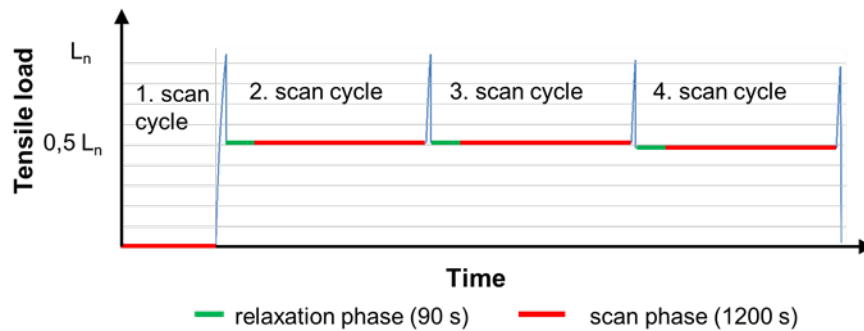


Figure 3. Basic procedure for in-situ CT examinations

4. Results

4.1. Void analysis

A void analysis was prepared in the first scan cycle without tensile loading. Figure 4 shows selected 3D tomograms specimens with low, middle and higher void content (V_v).

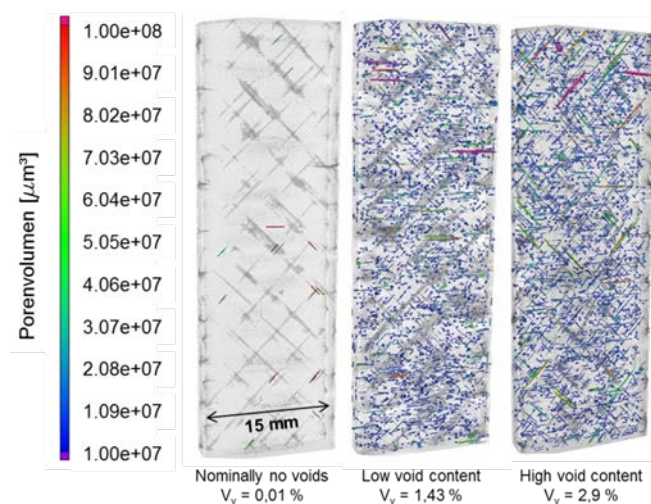


Figure 4. Typical 3D tomograms of nominal void-free (left), with few voids (centre) and many voids (right) of GF-NCF/EP specimens

In the nominal void-free test specimens ($V_v = 0.01\%$), isolated tube voids were detected between the fibre bundles of the 0° -layers and the 45° -layers. The determined average total void volume of $2.2 \times 10^8 \mu\text{m}^3$ corresponds to an average void volume content of 0.01% .

Samples with low void volume contents of 1.43% showed a homogeneous distribution of voids. With an average total volume of $3.7 \times 10^{10} \mu\text{m}^3$ voids, the majority of the voids have a void volume of less than $1 \times 10^7 \mu\text{m}^3$. In the fibre bundles of the outer layers, however, larger voids of 1.4×10^7 to $2.2 \times 10^7 \mu\text{m}^3$ were also detected in individual cases (Figure 5).

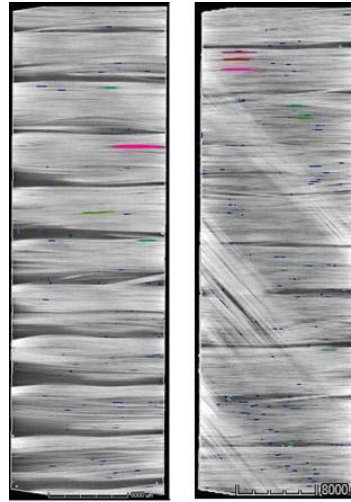


Figure 5. Highlighting of occasional larger voids in the 90°-layers

In the design of test specimens with a high void content, an average void volume content of 2.9 % with a total void volume of $2.0 \times 10^{12} \mu\text{m}^3$. Here, too, most voids have a volume of less than $1.0 \times 10^7 \mu\text{m}^3$. Larger voids from 1.2×10^7 to $1.5 \times 10^7 \mu\text{m}^3$ were detected in both the 0°-layers and the 45°-layers (Figure 6).

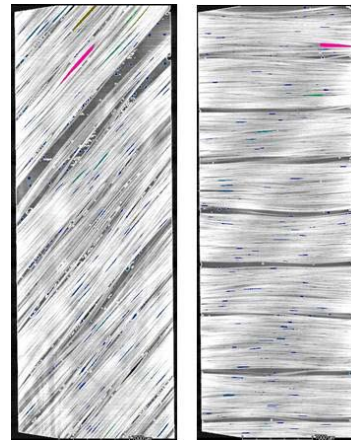


Figure 6. Highlighting of occasional larger voids in the 0°- and 45°-layers

The different void contents of the three designs are also clearly visible in the micrographs in Figure 7. The reference sample (left) is almost defect free, only smaller voids are visible. Large spherical voids in the intermediate fibre regions and smaller voids in the fibre regions are visible in samples with low void volume content. The samples with higher void volume content have significantly more voids across the cross-section but above all larger voids in the fibre bundles. In the upper 0°-layer, tube voids are often visible which orient themselves in the direction of the fibres. However, the majority of the voids can be found in the 45°-layers.

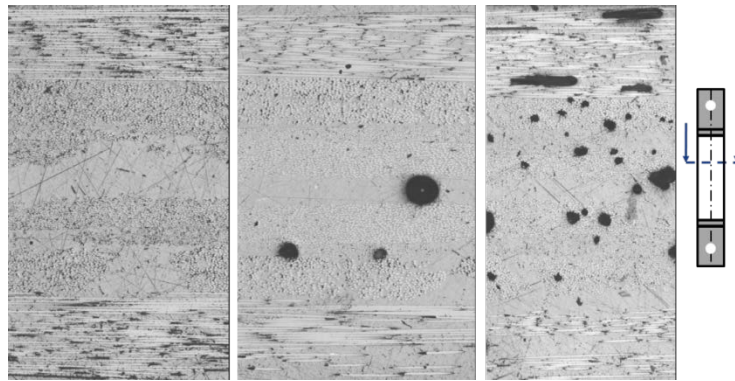


Figure 7. Selected micrographs for nominal void-free (left), with few voids (centre) and many voids (right) from GF-NCF/EP specimens

4.2. *In-situ CT*

The influence of voids on material mechanical behaviour was investigated with the aid of an in-situ CT. In favour of a more precise analysis of the fibres and voids, the known phenomena for the formation of inter-fibre breaks and delaminations under quasistatic tensile loading were not considered.

In the nominal defect free (low void content) reference samples, after the first force drop of 0.2 %, a first crack appears in a fibre bundle starting from the left edge, of the individual layer lying in the direction of loading. If the crack is located at a point where the fibre strands of the individual layers touch, the crack propagates parallel to the fibre orientation of the adjacent layer. From scan cycle to scan cycle a zigzag growth of this crack can be observed. The fibre strand also tears from the opposite side, as individual filaments break. Further cracks become visible in the adjacent fibre bundle, which increase until the sample fails (Figure 8). The individual voids detected in the sample do not initiate any cracks themselves and influence the load-induced crack propagation in the reference test piece. Crack initiation always occurs from the outside to the inside until a large part of the rovings in the load direction is damaged to such an extent that the load can no longer be transferred. The location of the cracks and the location of the final specimen failure are spontaneous and unpredictable in the sense of this investigation.

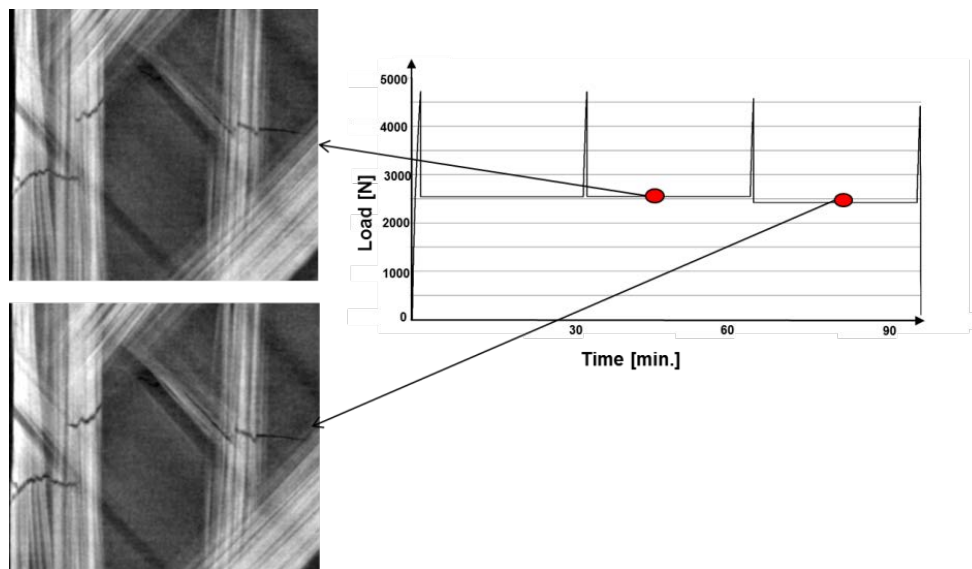


Figure 8. Typical crack progression in low-void reference specimen under tensile load

For the specimens examined here with void contents of 1.43 % and 2.90 %, the crack formation is far from the location of the largest void. Figure 9, for example, shows the three individual layers with the largest voids of a sample with a low void volume fraction detected by the CT software in the upper third of the test piece in pink. The two sectional images on the right show the crack formation locations removed from these voids.

Even with higher void contents, no correlation between the positions of the largest void and the location of crack formation can be seen (Figure 10).

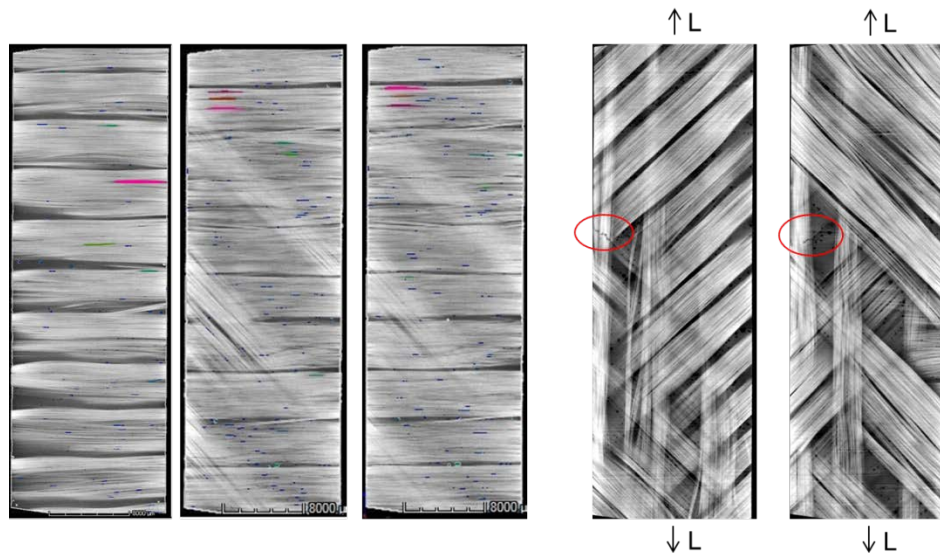


Figure 9. Location of the largest voids in GF-NCF/EP composites with low void content

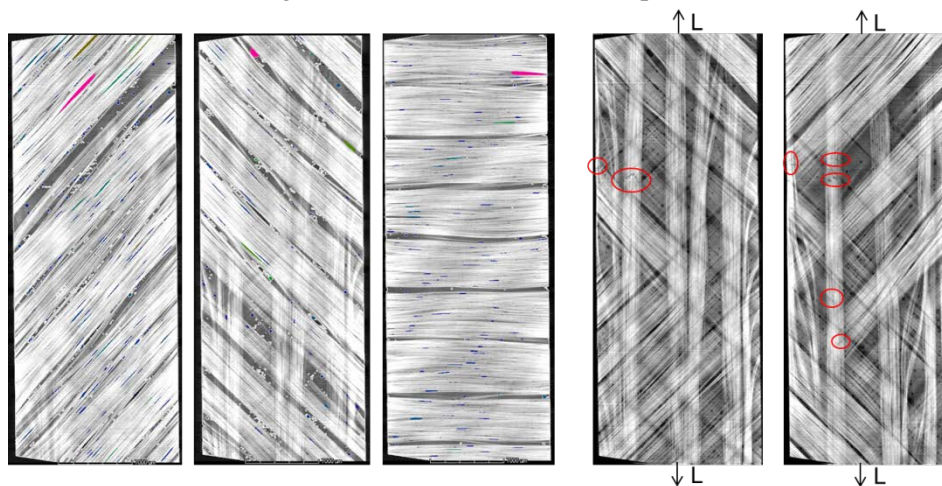


Figure 10. Location of the largest voids in GF-NCF/EP composites with high void content

In the analysis of selected individual inter-fibre cracks, the influence of voids cannot be excluded beyond all doubt. Cracks can be observed in various cases which migrate unhindered through void-rich regions and are neither deflected to the nearest void nor stopped by voids (Figure 11). The crack path is furthermore influenced by the orientation of the fibre bundles. Only in resin rich areas, where the crack usually is oriented perpendicular to the loading direction, selected cracks are influenced by voids. However, there are examples where voids act as crack stoppers or crack formation could be observed in the immediate vicinity of voids (Figure 12).

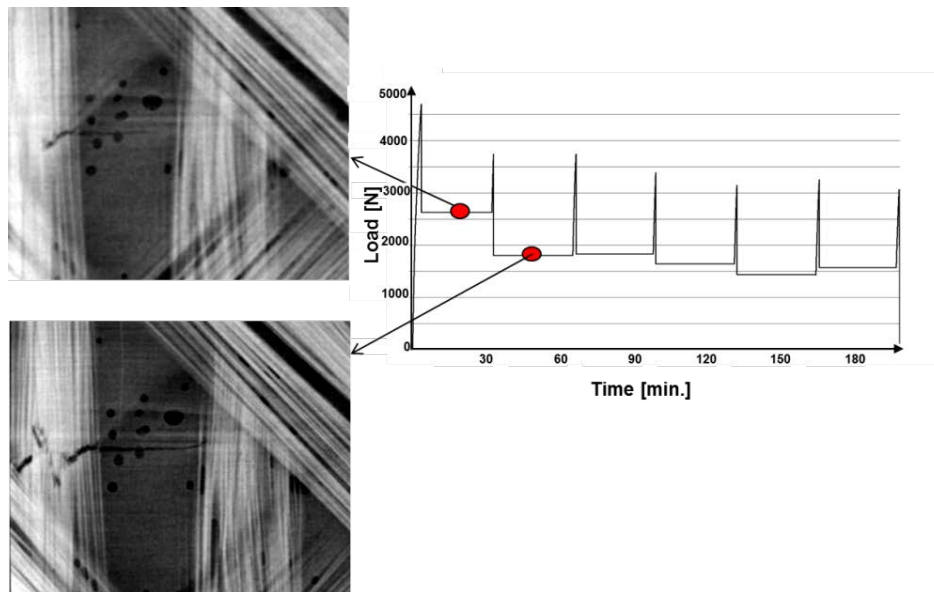


Figure 11. Example for voids not influencing the crack progression

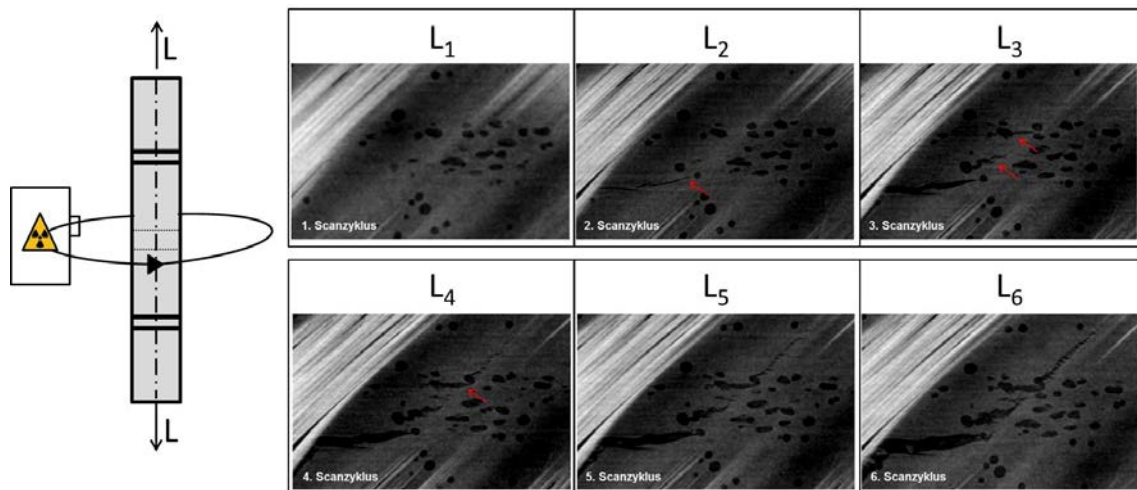


Figure 12. Example for voids acting as crack stoppers and source of cracks

5. Conclusion

An in-situ CT methodology was applied to determine the influence of voids on the damage behaviour of non-crimp glass fibre reinforced composites under tensile loading. It was found, that in samples with low void volume content cracks are initiated under tensile stress and their growth is not influenced by voids. As the void content increases, the cracks are increasingly deflected from existing voids. In the case of pointed tube voids, crack initiation indicates stress concentration in the vicinity of the void. However, also positive effects have been found as the growth of cracks may be stopped by spherical voids.

Acknowledgments

The authors gratefully acknowledge the financial support within the scope of research project PAK 267 “Effects of Defects” by the Deutsche Forschungsgemeinschaft (DFG).

References

- [1] Hufenbach W, Gude M and Ebert C 2006 Tailored 3D-textile reinforced composites with load adapted property profiles for crash and impact applications *Composites* **6** (3) 8-13.
- [2] Hufenbach W, 2007 editor. Textile Verbundbauweisen und Fertigungstechnologien für Leichtbaustrukturen des Maschinen- und Fahrzeugbaus Dresden: Progress media-Verlag, ISBN 978-3-00-022109-5.
- [3] Kosmann N, Karsten JM, Schuett M, Schulte K and Fiedler B 2015 Determining the effect of voids in GFRP on the damage behaviour under compression loading using acoustic emission *Compos Part B* **70** 184-8.
- [4] Rheinfurth M, Kosmann N, Sauer D, Busse G and Schulte K 2012 Lamb waves for noncontact fatigue state evaluation of composites under various mechanical loading conditions *Compos A Appl Sci Manuf* **43** (8) 1203-11.
- [5] Hufenbach W, Gude M and Protz R 2012 Modeling of the strain rate dependent material behavior of 3D-textile composites with production and operational defects. *Adv Mat Res* **403-408** 651-5.
- [6] Varna J, Joffe R, Berglund LA and Lundström TS 1995 Effect of voids on failure mechanisms in RTM laminates *Compos Sci Technol* **53** 241-9.
- [7] Liu L, Guo ZS and Zhang B 2006 Experimental investigation of porosity and its effects on interlaminar shear strength in composite laminates In: *SAMPE 2006-Long Beach, CA*.
- [8] Talreja R 2006 Effects on manufacturing induced defects on composite damage and failure. In: *The 27th Riso International Symposium: Polymer Composite Materials for Wind Power Turbines* 83-96.
- [9] Kaleta J, Blazejewski W, Gasior P and Rybaczuk M 2010 Optimization of the IV generation tanks for hydrogen storage applied in vehicles. Modelling and experiment. In: *Proceedings of the WHEC* 25-31.
- [10] Lundström TS and Gebart BR 1994 Influence from process parameters on void formation in resin transfer molding *Polym Compos* **15** (1) 25-33.
- [11] Afendi Md, Banks WM and Kirkwood D 2005 Bubble free resin for infusion process *Compos Part A* **36** 739-46.
- [12] Binetruy C, Hilaire B and Pabiot J 1998 Tow impregnation model and void formation mechanisms during RTM *J Compos Mater* **32** (3) 223-45.
- [13] Patel N, Rothatgi V and Lee J 1995 Micro scale flow behavior and void formation mechanism during impregnation through a unidirectional stitched fiberglass mat *Polym Eng Sci* **35** (10) 837-51.
- [14] Kang MK, Woo L and Hahn HT 2000 Formation of microvoids during resintransfer molding process *Compos Sci Technol* **60** 2427-34.
- [15] Lee DH, Lee WI and Kang MK 2006 Analysis and minimization of void formation during resin transfer molding process *Compos Sci Technol* **66** 3281-9.
- [16] Pujol S, Johnson MS, Warrior NA, Kendall KN and Hill DJ 2007. The effects of processing parameters on reactive epoxy adhesives. In: *16th International Conference on Composite Materials* 1-9.
- [17] Rius E, Achim V, Soukane S, Trochu F and Breard J 2006 Optimization of injection flow rate to minimize micro/macro-voids formation in resin transfer molded composites *Compos Sci Technol* **66** 475-86.
- [18] Howe CA, Paton RJ and Goodwin AA 1997 A comparison between voids in RTM and prepreg carbon/Epoxy laminates. In: *Proceedings of ICCM11, Gold Coast, Australia*.
- [19] Lambert J, Chambers AR, Sinclair I and Spearing SM 2012 3D damage characterisation and the role of voids in the fatigue of wind turbine blade materials *Compos Sci Technol* **72** 337-43.
- [20] Olivier AP, Mascaro B and Margueres P 2007 CFPR with voids: ultrasonic characterization of localized porosity, acceptance criteria and mechanical characteristics *16. ICCM, Japan*.

- [21] Chamber AR, Earl JS, Squires CA and Suhout MA 2006 The effect of voids on the flexural fatigue performance of unidirectional carbon fibre composites developed for wind turbine applications *Int J Fatigue* **28** 1389-98.
- [22] De Almeida SFM and Neto ZSN 1994 Effect of void content on the strength of composite laminates *Compos Struct* **28** (2) 139-48.
- [23] Browning CE 1986 Processing science of graphite/epoxy composites *Chem Eng Prog* **82** 41-9.
- [24] Huang H and Talreja R 2005 Effects of void geometry on elastic properties of unidirectional fiber reinforced composites *Compos Sci Technol* **65** 1964-81.
- [25] Schmidt F, Rheinfurth M, Horst P and Busse G 2012 Multiaxial fatigue behaviour of GFRP with evenly distributed or accumulated voids monitored by various NDT methodologies *Int J Fatigue* **43** 207-16.
- [26] Guo Z, Liu L, Zhang B and Du S 2009 Critical void content for thermoset composite laminates. *J Compos Mater* **43** (17) 1775-90.
- [27] Jeong H 1997 Effects of voids on the mechanical strength and ultrasonic attenuation of laminated composites *J Compos Mater* **31** 276-92.
- [28] Bowles KJ and Frimpong S 1992 Void effects on the interlaminar shear strength of unidirectional graphite-fibre-reinforced composites. *J Compos Mater* **26** 1487-509.
- [29] Rohatgi V, Patel N and Lee LJ 1996 Experimental investigation of flow-induced microvoids during impregnation of unidirectional stitched fiberglass mat *Polym Compos* **17** (2) 161-70.
- [30] Protz R, Kosmann N, Gude M, Hufenbach W, Schulte K and Fiedler B 2015 Voids and their effects on the strain rate dependent and fatigue damage behaviour of non-crimp fabric composites. *Composites B* **83** 346-351.
- [31] Protz R, Kosmann N, Fritsch D, Fey P, Adebahr W, Dietrich K, Gude M, Horst P, Kreutzbruck M, Schulte K, Busse G, Hufenbach W and Fiedler, B 2016 Influence of voids and impact damage on the fatigue behaviour of large scale composites *Mat.-wiss. u. Werkstofftech.* **47**, No. 11 1058-71.
- [32] Böhm R, Stiller J, Behnisch T, Zscheyge M, Protz R, Radloff S, Gude M and Hufenbach W 2015 A quantitative comparison of the capabilities of in situ computed tomography and conventional computed tomography for damage analysis of composites *Composites Science and Technology*, **110**, 62-68.
- [33] Maragoni L, Carraro PA, Peron M and Quaresimin M 2017 Fatigue behaviour of glass/epoxy laminates in the presence of voids *International Journal of Fatigue* **95** 18-28.
- [34] Maragoni L, Carraro PA and Quaresimin M 2016 Effect of voids on the crack formation in a [45/-45/0]_s laminate under cyclic axial tension *Composites A* **91** 493-00.
- [35] Schmidt F, Rheinfurth M, Horst P and Busse G 2012 Multiaxial fatigue behaviour of GFRP with evenly distributed or accumulated voids monitored by various NDT methodologies *International Journal of Fatigue* **43** 207-16.
- [36] Kosmann N, Karsten JM, Schuett M, Schulte K, and Fiedler B 2015 Determining the effect of voids in GFRP on the damage behaviour under compression loading using acoustic emission *Composites B* **70** 184-88.